

$\text{Fe}_3\text{O}_4@ \text{GdF}_3:\text{Er}^{3+}, \text{Yb}^{3+}$ nanoparticles: synthesis and bifunctional properties

GUIXIA LIU*, HONGXIA PENG, JINXIAN WANG, XIANGTING DONG

School of Chemistry and Environmental Engineering, Changchun University of Science and Technology, Changchun 130022, China.P.R.China

The core-shell structured bifunctional magnetic and up-conversion fluorescence nanoparticles composed of Fe_3O_4 magnetic core and $\text{GdF}_3:\text{Er}^{3+}, \text{Yb}^{3+}$ up-conversion fluorescent shell were fabricated by a facile direct precipitation method. X-ray diffraction (XRD), Fourier transform infrared spectroscopy (FTIR), transmission electron microscopy (TEM), photoluminescence (PL), and superconducting quantum interface device (SQUID) were employed to characterize the samples. The results show that the composite nanoparticles are core-shell structures and have a typical diameter of 60 nm consisting of the magnetic core with about 40 nm in diameter and up-conversion fluorescent nanocrystals with an average thickness of about 15–20 nm. They possess magnetism with a saturation magnetization of 6.98 emu/g and exhibit green and red emissions originating from electric transition $^4\text{S}_{3/2} - ^4\text{I}_{15/2}$ (543 nm) and $^4\text{F}_{9/2} - ^4\text{I}_{15/2}$ (659 nm) of Er^{3+} ions. These results suggest that the bifunctional magnetic and up-conversion fluorescence nanocomposites with magnetic resonance response and up-conversion fluorescence probe property may be useful in biomedical imaging and diagnostic applications.

(Received February 25, 2012; accepted April 11, 2012)

Keywords: Fe_3O_4 , $\text{GdF}_3:\text{Er}^{3+}, \text{Yb}^{3+}$, Core-shell, Magnetism, Up-conversion fluorescence

1. Introduction

Multi-functional nanocomposites that possess desirable properties in a single entity have attracted great interest in recent years. For instance, nanocomposites with both fluorescent and magnetic properties can be used in biological systems, such as bioimaging, diagnostic, and therapeutics.¹⁻⁴ They can serve as fluorescent markers, at the same time, they can also be controlled by an external magnetic field.⁵⁻⁸ Most of the magnetic fluorescent nanocomposites are core-shell structures with the great majority of emitters being either quantum dots (QDs) or organic dyes.⁹⁻¹²

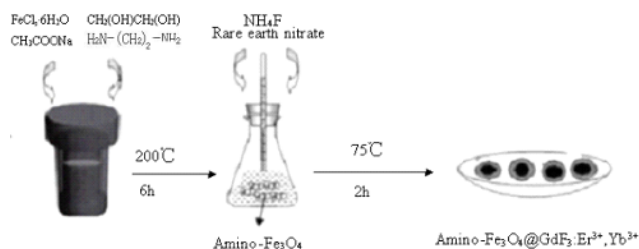
However, organic dyes typically exhibit rapid photobleaching and a low fluorescence quantum yield, QDs are less chemically stable, potentially toxic, and show fluorescence intermittence.^[13-15] Therefore, such intrinsic disadvantages would seriously hinder their application in the biomedical field, especially for use in the human body.¹⁶⁻¹⁸ Recently, lanthanide-doped upconversion nanocrystals have been developed as a new class of luminescent labels, and they have become promising alternatives to organic fluorescent dyes or quantum dots for applications in biological assays and medical imaging,^{19,20} due to their attractive chemical and optical features, such as large anti-stokes shifts, low toxicity, sharp absorption, emission lines and superior photostability. In particular, up-conversion luminescence is a process that continuous-wave low-energy light in the near-infrared (NIR) region (typically 980 nm) is converted to higher energy visible light through sequential absorption of

multiple photons or energy transfer,^{21,22} and such a unique luminescent mechanism excludes both conventional luminescent labels and endogenous fluorescent substances.^{23,24} Therefore, it can be expected that upconversion nanocrystals may exhibit many advantages, such as non-invasive and deep penetration of NIR radiation, probable absence of auto fluorescence of biological tissues, and the low cost of continuous-wave NIR laser.²⁵⁻²⁸ They have recently been used as luminescent labels for bioimaging. Rare-earth fluorides are a class of materials with great potential in optical applications. Fluoride lattices allow high coordination numbers for the host rare-earth ions,²⁹ the high ionicity of the rare-earth-to-fluorine bond leads to a wide bandgap and very low vibrational energies.^{30,31} These two factors in particular contribute to their usability in optical applications based on vacuum ultraviolet (VUV) and near-infrared (NIR) excitation.³²

Several different routes have been used to synthesize bifunctional magnetic luminescent nanocomposites. Fang et al. employed a facile one-pot method to fabricate the $\text{Fe}_3\text{O}_4@ \text{SC}[6]-\text{LaPO}_4:\text{Ce}^{3+}, \text{Tb}^{3+}$ superparamagnetic and fluorescent nanocomposites. The $\text{LaPO}_4:\text{Ce}^{3+}, \text{Tb}^{3+}$ nanorods were self-assembled into three-dimensional “koosh nanoballs” as a bifunctional luminescent ferro-fluidic system.³³ Sun et al. had synthesized $\text{Fe}_3\text{O}_4/\text{SiO}_2/\text{YVO}_4:\text{Eu}^{3+}$ magnetic/luminescent nanocomposites by a hydrothermal method.³⁴ Lu et al. employed a modified Stöber method combined with a layer-by-layer assembly technique to fabricate the core-shell structured luminomagnetic microsphere composed of a Fe_3O_4 magnetic core and a continuous SiO_2

nanoshell doped with $\text{Eu}(\text{DBM})_3 \cdot 2\text{H}_2\text{O}$ fluorescent molecules. This obtained luminescent microspheres with magnetic resonance response and fluorescence probe property may be useful in biomedical imaging and diagnostic applications.³⁵ Zhang et al. had prepared $\text{Fe}_3\text{O}_4 @ \text{SiO}_2 / \text{Y}_2\text{O}_3 : \text{Tb}$ bifunctional nanocomposites by homogeneous precipitation method.³⁶ To the best of our knowledge, there are few reports on the synthesis of bifunctional magnetic and up-conversion luminescent nanocomposites with Fe_3O_4 nanoparticles as the cores and lanthanide-doped fluoride nanoparticles as the shells.

In this work, we report the development of a facile two-step method for the preparation of bifunctional magnetic and up-conversion luminescent nanocomposites. First, amino-functional magnetic Fe_3O_4 nanoparticles were solvothermally prepared as the cores. Second, amino-functional Fe_3O_4 nanoparticles coated with $\text{GdF}_3 : \text{Er}^{3+}, \text{Yb}^{3+}$ up-conversion luminescent particles as the shells were synthesized by a direct precipitation method. The synthetic strategy as schematically illustrated in Scheme 1. With the excellent magnetic properties and surface amino functional groups of Fe_3O_4 cores, $\text{GdF}_3 : \text{Er}^{3+}, \text{Yb}^{3+}$ can be successfully deposited on their surface, so $\text{Fe}_3\text{O}_4 @ \text{GdF}_3 : \text{Er}^{3+}, \text{Yb}^{3+}$ are synthesized. The prepared product has green and red up-conversion emission and magnetic property.



Scheme 1. Synthetic route of $\text{Fe}_3\text{O}_4 @ \text{GdF}_3 : \text{Er}^{3+}, \text{Yb}^{3+}$ bifunctional composite nanoparticles

2 experimental details

2.1 Materials

Gadolinium oxide (Gd_2O_3 , purity:99.99%), ytterbium oxide (Yb_2O_3 ,99.99%) and erbium oxide (Er_2O_3 , 99.99%) were purchased from Shanghai Yuelong Non-Ferrous Metal Limited, China, Ammonium fluoride (NH_4F , purity: 96.0%), Ferric chloride hexahydrate ($\text{FeCl}_3 \cdot 6\text{H}_2\text{O}$, purity \geq 99.0%), ethylenediamine ($\text{C}_2\text{H}_8\text{N}_2$, purity \geq 98.0%), sodium acetate (CH_3COONa , purity \geq 99.0%), Ethylene glycol (EG, purity 96.0%) were purchased from Beijing Chemical Reagent Limited, China. All chemicals were used without any further purification. Deionized water was used throughout.

2.2 Characterization

Powder XRD patterns were obtained on a Bruker D&FOCUS X-ray powder diffraction (XRD) using $\text{Cu-K}\alpha$

radiation ($\lambda=0.154056$ nm). The morphologies and structures of the as-prepared samples were inspected on a JEM-2010-type transmission electron microscope (TEM). The upconversion emission spectra of samples were performed with a Hitachi F-4500 fluorescence spectrometer. An adjustable laser diode (980 nm, 2 w) was used as the excitation source. Magnetization measurements were performed on an MPMS SQUID XL superconducting quantum interference device (SQUID) magnetometer at 300 K. All the measurements were performed at room temperature.

2.3 Synthesis of amino-functional magnetic Fe_3O_4 nanoparticles

Amino-functional magnetic Fe_3O_4 nanoparticles were prepared by the solvent-thermal method.³⁷ Briefly, $\text{FeCl}_3 \cdot 6\text{H}_2\text{O}$ (1.0 g) was dissolved in ethylene glycol (30 mL) to form a clear solution, followed by the addition of NaAc (2.0 g) and ethylenediamine (6.5 g). The mixture was stirred vigorously for 30 min and then sealed in a teflon-lined stainless-steel autoclave (50 mL capacity). The autoclave was heated to and maintained at 200 °C for 6 h, and then cooled to room temperature naturally. The black products were washed several times with ethanol and finally dried at 60 °C for 6 h.

2.4 Synthesis of $\text{Fe}_3\text{O}_4 @ \text{GdF}_3 : \text{Er}^{3+}, \text{Yb}^{3+}$ nanocomposites

$\text{Er}^{3+}, \text{Yb}^{3+}$ -doped gadolinium fluoride ($\text{GdF}_3 : \text{Er}^{3+}, \text{Yb}^{3+}$) luminescent shell was coated on the magnetic Fe_3O_4 nanoparticles by a direct precipitation method. The detailed procedure was as follows: First, gadolinium oxide, ytterbium oxide and erbium oxide were respectively dissolved in a minimum amount of diluted nitric acid (1:1), evaporated to dryness, cooled to room temperature, then dissolved in distilled water to form 0.2 mol/L of gadolinium nitrate, ytterbium nitrate and erbium nitrate solutions. Secondly, 0.2 g of as-prepared Fe_3O_4 nanoparticles were dispersed in 16 mL of $\text{Gd}(\text{NO}_3)_3$, 0.8 mL of $\text{Er}(\text{NO}_3)_3$ and 4.5 mL of $\text{Yb}(\text{NO}_3)_3$ solutions. The mixture was sonicated for 20 min followed by the addition of 21 mL of NH_4F (0.6 mol/L) solution, and then heated to 75 °C under vigorous mechanical stirring. After 2 h, the resultant products were separated with a magnet, thoroughly washed with ethanol and deionized water several times, and further dried at 60°C overnight.

3. Results and discussion

3.1 Morphologies of the samples

Fe_3O_4 particles prepared by a solvothermal process, consist of spherical nanoparticles with an average diameter of about 40 nm, a smooth surface and apparent aggregation (Fig. 1a). The $\text{Fe}_3\text{O}_4 @ \text{GdF}_3 : \text{Er}^{3+}, \text{Yb}^{3+}$

particles are also in spherical morphology, with non-aggregation and rough surface (Fig. 1b,c).

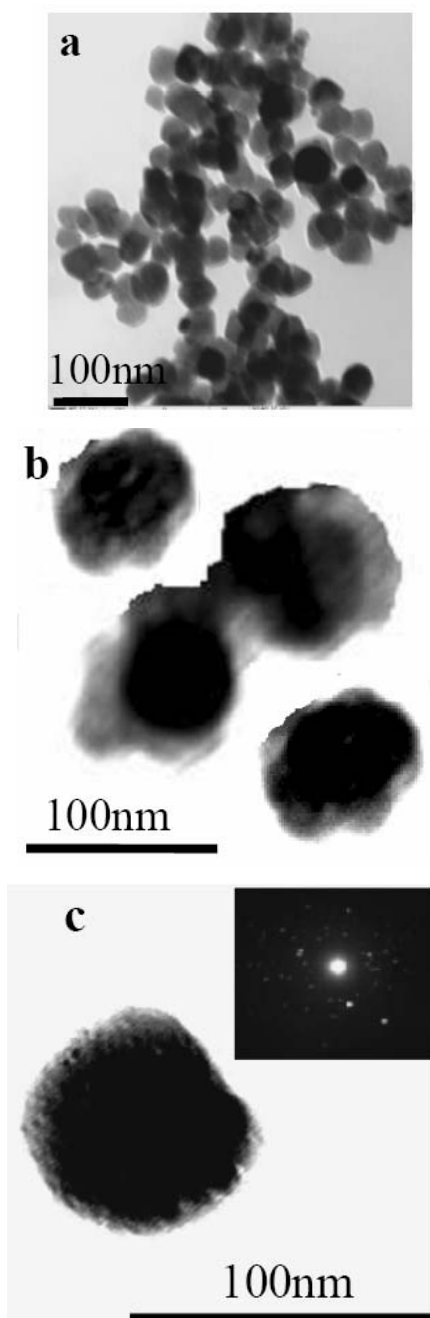


Fig. 1 TEM images of the samples (a) Fe₃O₄ (b,c) Fe₃O₄@GdF₃:Er³⁺,Yb³⁺

In addition, the core-shell structure can be clearly distinguished because of the different color contrast between the cores and shells. Fe₃O₄@GdF₃:Er³⁺,Yb³⁺ are spheres with an average size of about 60 nm, and the shell shows a gray color with an average thickness of about 15~20 nm (Fig. 1b and 1c). The change in diameter in Fig. 1a and c suggests that the GdF₃ nanocrystal deposited on the surface of Fe₃O₄ nanoparticles. The selected-area electron diffraction (SAED, the inset of Fig. 1c) reveals

the polycrystalline feature of the as-prepared product.

3.2 Structure of the samples

In order to investigate the structure and composition of the nanocomposites, XRD was employed to analyze the samples. Fig. 2 shows the X-ray diffraction patterns of Fe₃O₄ and Fe₃O₄@GdF₃:Er³⁺,Yb³⁺ particles. From Fig 2a, it is found that the magnetite core is easily indexed to cubic spinel structure of Fe₃O₄ (PDF 75-1610) with good crystallinity. Fig. 2b shows that the nanocomposites exhibit the characteristic diffraction peaks of GdF₃ (PDF 12-0788) with orthogonal phase and additional peaks that coincide with the peaks of cubic spinel Fe₃O₄ (marked with *) and γ -Fe₂O₃ (marked with °). The coexistence of maghemite and magnetite could be attributed to oxidation of Fe₃O₄ to γ -Fe₂O₃ during the synthesis.²⁶ The XRD results indicate the successful crystallization of GdF₃:Er³⁺,Yb³⁺ on the surface of Fe₃O₄. Additionally, no additional peaks for other phases can be detected, indicating that no reaction occurred between the core and shell during the synthesis process.

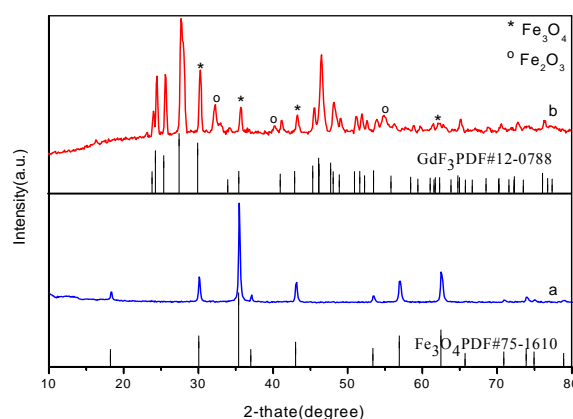


Fig.2 XRD patterns of the samples (a) Fe₃O₄; (b) Fe₃O₄@GdF₃:Er³⁺,Yb³⁺

3.3 Fluorescence properties of the bifunctional nanocomposites

After the magnetic nanoparticle was coated with GdF₃:Er³⁺, Yb³⁺, green and red up-conversion emissions were observed with 980 nm infrared excitation. Fig.3 shows the infrared-to-visible up-conversion fluorescence spectrum of the sample. The two emission peaks at 543 and 659 nm, assigned respectively to ⁴S_{3/2} to ⁴I_{15/2} and ⁴F_{9/2} to ⁴I_{15/2} transition of erbium, are similar to the emission peaks observed in previous report for the pure up-conversion nanoparticle itself.³⁸ In addition, the spectrum shows that the red ⁴F_{9/2} - ⁴I_{15/2} emission (659 nm) is stronger than the green ⁴S_{3/2} - ⁴I_{15/2} emission (543 nm) (emission ratio of red to green is 2:1). Because the surface properties and crystallinity of GdF₃:Er³⁺, Yb³⁺

nanoparticles can affect the different energy level transition of doped ions, then they result in the different emission intensity of red and green light. The up-conversion fluorescence property was still preserved when the material was coated as a shell on magnetic nanoparticles. These nanocomposites with up-conversion fluorescence have many optical advantages (e.g. low optical background, high photo-stability and low laser cost), and thus they can be employed as reporters in immunoassays or DNA assays.³⁹ Meanwhile, the existence of $\text{Fe}_3\text{O}_4/\gamma\text{-Fe}_2\text{O}_3$ may not obviously influence the fluorescence property of the nanocomposites.

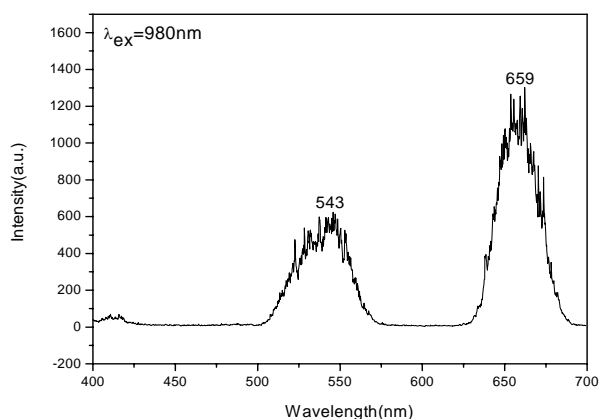


Fig.3 Upconversion emission spectrum of $\text{Fe}_3\text{O}_4@\text{GdF}_3:\text{Er}^{3+}, \text{Yb}^{3+}$ nanocomposites under the excitation of 980 nm laser

3.4 Magnetic properties of the bifunctional nanocomposites

Fig. 4 shows the magnetic properties of the Fe_3O_4 core and the $\text{Fe}_3\text{O}_4@\text{GdF}_3:\text{Er}^{3+}, \text{Yb}^{3+}$ nanocomposites. Both samples exhibit a magnetic behavior with a negligible coercivity or remanence, indicating that the as-prepared sample is suitable for applications in drug delivery or separation. The saturation magnetization of $\text{Fe}_3\text{O}_4@\text{GdF}_3:\text{Er}^{3+}, \text{Yb}^{3+}$ nanocomposites reaches a saturation moment of 6.98 emu/g, the value is much lower than that of Fe_3O_4 cores (88.58 emu/g), probably because of the thick shells coated on magnetic nanoparticles. Another main reason is that a part of Fe_3O_4 has been oxidized to $\gamma\text{-Fe}_2\text{O}_3$ during the synthesis from XRD results. Generally, surface oxidation of nanomaterials would significantly reduce the total magnetic moment, as compared to that of bulk materials. Nevertheless, this kind of magnetic property enables the bifunctional composite particles to be used in biomedical applications because they have a sufficiently strong magnetization for efficient magnetic separation under the applied external magnetic field.

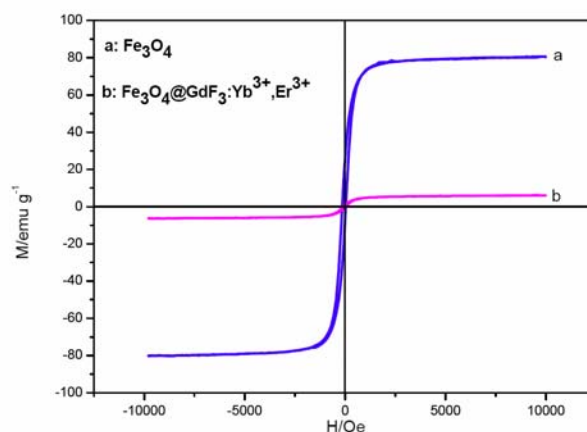


Fig. 4 Magnetization curves of Fe_3O_4 core (a) and $\text{Fe}_3\text{O}_4@\text{GdF}_3:\text{Er}^{3+}, \text{Yb}^{3+}$ nanocomposites (b) at room temperature.

4. Conclusions

In summary, we fabricated the $\text{Fe}_3\text{O}_4@\text{GdF}_3:\text{Er}^{3+}, \text{Yb}^{3+}$ magnetic and up-conversion fluorescence nanocomposites with a facile direct precipitation process. The nanocomposites simultaneously exhibit magnetic and up-conversion fluorescence properties. In a word, the magnetic and up-conversion fluorescence properties of the nanocomposites would allow them to find great potential applications in biomedical fields.

Acknowledgements

This work was supported by the National Natural Science Foundation of P.R. China (NSFC) (Grant No. 51072026, 50972020) and the Development of science and technology plan projects of Jilin province (Grant No. 20090528).

References

- [1] R. D. Corato, N. C. Bigall, A. Ragusa, D. Dorfs, A. Genovese, R. Marotta, L. Manna, T. Pellegrino, *ACS Nano*, DOI: 10.1021/nn102761t
- [2] H.M. Fan, M. Olivo, B. Shuter, J.B. Yi, R. Bhuvanewari, H. R.Tan, G.C. Xing, C.T. Ng, L. Liu, S. S. Lucky, B.H.Bay, J. Ding, *J. Am. Chem. Soc.* **132**,14803(2010)
- [3] P.P. Yang, Z.W. Quan, Z.Y. Hou, C.X. Li, X.J. Kang, Z.Y. Cheng, J. Lin, *Biomaterials*, **30**, 4786(2009)
- [4] J. Wu, Y.T. Yang, *J. Nanosci. Nanotechnol.*, **58**,1743(2008)
- [5] E.Q. Song, J. Hu, C.Y. Wen, Z. Q. Tian, X. Yu, Z.L. Zhang, Y.B. Shi, D.W. Pang, *ACS Nano*, Articles ASAP (As Soon As Publishable) DOI: 10.1021/nn1011336

- [6] S. T.Selvan, T.T. Y.Tan, D. K.Yi, N. R. Jana, *Langmuir*, **26**,14, 11631(2010)
- [7] Z. Y. Ma, D. Dosev, M. Nichkova, S. J. Gee, B. D. Hammock, I. M. Kennedy, *J. Mater. Chem* **19**, 4695(2009)
- [8] W.Q. Fan, J.Feng, S.Y. Song, Y.Q. Lei, Y. Xing, R.P. Deng, S. Dang, H.J. Zhang, *Eur. J. Inorg. Chem*, 5513(2008)
- [9] L. Wang, K.G. Neoh, E.T. Kang, B. Shuter, S.C. Wang, *Biomaterials*, **31**,3502(2010)
- [10] O. Veiseh, C. Sun, J. Gunn, N. Kohler, P. Gabikian, D. Lee, N. Bhattarai, R. Ellenbogen, R. Sze, A. Hallahan, J. Olson, M. Q. Zhang, *Nano Lett*, **5**, 6 (2005)
- [11] Z.T.Liu, C. Li, Y.P. Fu, Y. Yang, *J. Nanosci. Nanotechnol*, **79**, 3152(2007)
- [12] K.Y. Bao, S.Z. Liu, J. Cao, *J. Nanosci. Nanotechnol* **08**, 4918(2009)
- [13] Z.W. Sun, D.M. Liu, L.Z. Tong, J.H.Shi, X.W.Yang, L.X. Yu, Y.C.Tao and H. Yang, *Solid State Sciences* **132**, 361(2011)
- [14] M. Nichkova, D.Dosev, S. J. Gee, *Analytical Biochemistry* **369**,34(2007)
- [15] A. Son, D. Dosev, M. Nichkova, Z.Y. Ma, I. M. Kennedy, K. M. Scow, K. R. Hristov, *Analytical Biochemistry* **370**, 186 (2007)
- [16] L.Y. Wang, Z.H. Yang, Y. Zhang, L. Wang, *J. Phys. Chem. C* **113**, 3955(2009)
- [17] J. Choi, J. C. Kim, Y. B. Lee, I. S. Kim, Y. K. Park, N. H. Hur, *Chem. Commun*, 1644(2007)
- [18] H. He, M.Y. Xie, Y. Ding, X.F. Yu, *Applied Surface Science* **255**, 4623(2009)
- [19] F. Wang, X.G. Liu, *Chem. Soc. Rev* **38**, 976(2009)
- [20] L.Q. Xiong, Z.G. Chen, M.X. Yu, F.Y. Li, C. Liu, C.H. Huang, *Biomaterials* **30**, 5592(2009)
- [21] Q. Lu, F.Y. Guo, L. Sun, A.H.Li, L.C. Zhao, *J. Phys. Chem. C* **112**, 2836(2008)
- [22] G. K.Das, B. C. Heng, S.C.Ng, T. White, J. S.C. Loo, L. D. Silva, P. Padmanabhan, K. K. Bhakoo, S. T. Selvan and T.T. Y.Tan, *Langmuir* **26**(11), 8959(2010).
- [23] F. Vetrone, R. Naccache, V. Mahalingam, C. G. Morgan, J. A. Capobianco, *Adv. Funct. Mater* **19**, 1 (2009)
- [24] H. Wang, J. Yang, C.M. Zhang, J. Lin, *Journal of Solid State Chemistry*, **182**, 2716 (2009)
- [25] G.F.Wang, P. Wei, L.L. Wang, G.D. Wei, P. F. Zhu, D.S.Zhang, F.H. Ding, *J. Rare Earths* **272**, 330(2009)
- [26] S.L.Gai, P.P. Yang, C.X. Li, W.X.Wang, Y.L. Dai, N. Niu, J. Lin, *Adv. Funct. Mater*, 20,1166(2010)
- [27] H.R.Zheng, X.Y. Zhang, D. L. Gao, R. S. Meltzer, *J. Nanosci. Nanotechnol*, **83**, 1214(2010)
- [28] J. Ryu, H.Y. Park, K.Kim, H. Kim, J. H. Yoo, M. Kang, K. Im, R. Grailhe, R. Song, *J. Phys. Chem. C* **114**(49),21077(2010)
- [29] M. Darbandi and T.Nann,*Chem.Commun*, 776 (2006)
- [30] M. M. Lezhnina, T. Jüstel, H. Kätker, D.U. Wiechert, U. H. Kynast, *Adv. Funct. Mate* **16**, 935(2006)
- [31] P.Rahman, M. Green, *Nanoscale* **1**, 214(2009)
- [32] J.S.Zhang, W.P.Qin, J.S. Zhang, Y.Wan, C.Y..Cao, Y. Jin, G.D. Wei, G. F. Wang, L.L.Wang, *Chem. Res.Chinese*, **23**(6), 733(2007)
- [33] J.Fang, M.Saunders, Y.L. Guo, G.L. Lu, C. L. Raston, K. S. Iyer, *Chem. Commun*, **46**, 3074(2010)
- [34] P. Sun, H.Y. Zhang, C. Liu, J. Fang, M. Wang, J. Chen, J.P. Zhang, C.B. Mao and S.K. Xu, *Langmuir*, **262**, 1278(2010)
- [35] P. Lu, J. L. Zhang, Y.L. Liu, D.H. Sun, G.X. Liu, G.Y.Hong, J.Z. Ni, *Talanta*, **822**, 450(2010)
- [36] Y.X. Zhang, S.S. Pan, X.M. Teng, *J. Phys. Chem. C*, **2008**(112), 9623(2005)
- [37] H.Deng, X. L. Li, Q. Peng, *J. Angew.Chem.Int.Ed*, **44**, 2782(2005)
- [38] Y. Wang, W. P. Qin, J. S. Zhang, C.Y. Cao, J.S. Zhang, Y. Jin, *Journal of rare earths* **25**, 605(2007)
- [39] Y. Mita, H. Yamamoto, K. Katayanagi, S. Shionoya, *J. Appl. Phys* **78**, 1219 (1995).

*Corresponding author: liuguixia22@yahoo.com.cn